The outer limits of the lunar sodium exosphere

Jody K. Wilson, Jeffrey Baumgardner, and Michael Mendillo
Center for Space Physics, Boston Univ., USA

Received 31 March 2003; revised 9 May 2003; accepted 19 May 2003; published 27 June 2003.

[1] A new wide-angle coronagraphic-type imaging system used for the lunar eclipse of 16 July 2000 resulted in detections of the lunar sodium exosphere out to ~20 lunar radii, approximately twice the size recorded with narrower fields of view during previous eclipses. These measurements and subsequent modeling provide a unique constraint on the fastest atoms ejected from the lunar surface that form the lunar exosphere, indicative of the most energetic space weathering processes acting on the lunar surface. At most, only a small fraction of the atoms are ejected from the surface with speeds faster than escape speed of 2.4 km s^{-1}, meaning solar photon radiation pressure largely contributes to the escape of sodium atoms which form the comet-like tail. The total rate of sodium ejection from the surface for speeds >2.0 km s^{-1} is comparable to estimates from previous lunar eclipse observations and earlier images of the lunar sodium tail. *INDEX TERMS:* 6250 Planetology: Solar System Objects: Moon (1221); 6025 Planetology: Comets and Small Bodies: Interactions with solar wind plasma and fields; 6007 Planetology: Comets and Small Bodies: Atmospheres—structure and dynamics. **Citation:** Wilson, J. K., J. Baumgardner, and M. J. Mendillo, The outer limits of the lunar sodium exosphere, *Geophys. Res. Lett.*, *30*(12), 1649, doi:10.1029/2003GL017443, 2003.

1. Introduction

[2] The lunar exosphere is composed of atoms liberated from the lunar surface via interactions with sunlight, the solar wind, and meteorite bombardment. The relative importance of these processes is uncertain, though considerable progress has been made in the last decade [*Stern*, 1999]. One method of distinguishing exospheric source mechanisms is by determining the speed distribution of the atoms within the exosphere, since each process results in its own unique speed distribution of atoms ejected from the surface. Previous observations of Na atoms in the exosphere within 1000 km or so of the lunar limb [e.g., *Potter and Morgan*, 1988, 1991, 1998; *Tyler et al.*, 1988; *Hunten et al.*, 1991, 1998; *Sprague et al.*, 1992, 1998; *Stern and Flynn*, 1995; *Contarini et al.*, 1996; *Cremonese and Verani*, 1997; *Potter et al.*, 2000, *Verani et al.*, 2001] have been useful in measuring the atoms at the low end of the speed distribution, since these atoms move at well below the escape speed of 2.4 km s^{-1} and therefore remain close to the surface in ballistic trajectories. On the other hand, it is more difficult to quantify the exospheric component that includes atoms at speeds close to or above the escape speed. These atoms yield close to a r^{-1} radial brightness profile, where r is the distance from the center of the Moon, for a wide range of speeds. In order to determine the highest speeds in the lunar exosphere, a way is needed to follow the trajectories of these escaping atoms. The most straightforward solution is to image the outermost limits of the exosphere on a larger spatial scale than in any previous measurements. An eclipse in July 2000 provided the opportunity to accomplish exactly this.

2. Data

[3] We observed the Moon during an exceptionally long (107 minute) lunar eclipse on 16 July 2000 from a remote site near Cairns, Australia. We acquired images using a small telescope with a 45° field of view and an intensified CCD camera. An occulting mask at the first image plane blocked the lunar disk in order to reduce scattered light within the telescope. As with previous eclipse observations that used only a 6° field of view [*Mendillo and Baumgardner*, 1995; *Mendillo et al.*, 1999], we used narrow-band filters to isolate the emission of Na atoms from any solar continuum light reflecting off of the Moon. The telescope is a variation of our wide field all-sky cameras used for terrestrial airglow imaging [*Baumgardner et al.*, 1993], with the interference filters located in a collimated beam. Due to different angles of incidence on the filters for different locations in the observed field, the total transmission of the two Na D lines (5890, 5896 Å) varies by ~5% over the entire field of view, and we correct for this using images of a Na lamp-illuminated flat-field.

[4] Images are dark-subtracted and divided by flat fields. Off-band images are subtracted from on-band (Na) images to yield only the emission from Na atoms in the lunar exosphere and the Earth's mesosphere. Standard stars in the field of view are used for absolute intensity calibration. The Earth's Na emission was approximately uniform over the field, and we subtract this value from each pixel in the image. The Earth's penumbra was located entirely within the field of the occulting mask, so there is no need to correct for partial solar illumination in the data.

[5] The final reduced image in Figure 1 shows that the lunar Na exosphere appears to extend at least 20 lunar radii (R_M) from the Moon, but it is important to note that we are essentially looking head-on at the lunar exosphere and comet-like Na tail. The Na atoms in these images are mostly escaping, accelerated away from the Sun (and the Earth, in this geometry) by radiation pressure into an anti-sunward tail. That the exosphere appears to have a limited extent is not entirely due to gravitational effects of the Moon; it is also due to the initial launch velocities of the Na atoms, combined with projection effects as the atoms accelerate towards the "vanishing point" of the lunar Na tail in the anti-sunward direction [e.g., *Wilson et al.*, 1999].

0094-8276/03/2003GL017443$05.00

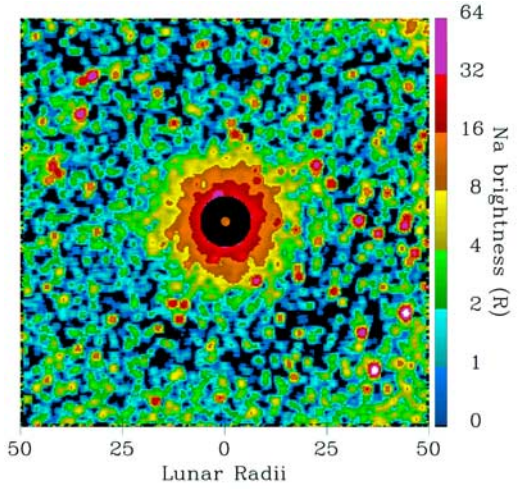

Figure 1. Image of the lunar Na exosphere during total lunar eclipse of 16 July 2002. The field of view spans 25° on a side. The center of the image is covered by the occulting mask (black). A separate image of the disk of the Moon has been added for scale.

[6] The apparent extent of the lunar Na exosphere is indicative of the highest ejection speeds of the Na atoms from the lunar surface - these are the atoms which achieve the highest apparent angular distance from the Moon before their motion is dominated by down-tail acceleration. These ejection speeds, in turn, are indicative of the mechanisms that liberated the atoms from the surface. The relative importance of the various candidate mechanisms has yet to be determined empirically, so it is useful to determine as precisely as possible the actual velocity distribution within the lunar exosphere. Observations very close to the lunar limb have been able to measure the low-energy regions of the distribution; however, no previous observations have been as sensitive to the high-energy region as those presented in Figure 1.

3. Modeling

[7] We simulate the lunar Na exosphere with a numerical/Monte-Carlo model to determine both the speed distribution and escape rate of the atoms that can form the vast exospheric region shown in Figure 1. Atoms ejected from the lunar surface with speeds below $\sim$2 km s^{-1} do not reach sufficient heights above the Moon to be seen in our images, so we do not attempt to characterize them here.

[8] The model uses a Monte-Carlo method to assign launch locations and velocities to simulated atoms, and uses fourth-order Runge-Kutta integration to calculate the subsequent trajectories. The gravitational fields of the Moon, Earth, and Sun are included, as is solar radiation pressure. A nominal Na photoionization lifetime of 42 hours is adopted [*Huebner*, 1992; *Combi et al.*, 1997; *Cremonese and Verani*, 1997], and new ions are removed from the simulation since they are invisible in our images and are quickly carried away by the solar wind.

[9] The model accounts for the increased ionization lifetime and reduced radiation pressure in the Earth's penumbra and umbra due to the reduced photon flux there, however the overall effect on the Moon's exosphere is small. A given point on the Moon's surface spends less than 3 hours in the umbra during the eclipse, or $\sim$7% of the nominal photoionization lifetime. A Na atom in full sunlight experiences a velocity change of $\sim$0.3 km s^{-1} in 3 hours, resulting in an anti-sunward displacement of $\sim$1 R_M, which is small compared to the extent of the exosphere seen in Figure 1.

[10] When interpreting the exospheres generated by the model, it is important to distinguish the nominal escape speed from the lunar surface (2.4 km s^{-1}) from the Na atom launch speeds which, with the help of solar radiation pressure, actually result in escaping Na atoms. Sodium atoms ejected from the surface with speeds above $\sim$2.0 km s^{-1}, but below the escape speed, can still escape directly from the Moon thanks to the boost given by radiation pressure. Atoms launched directly towards the Sun simply end up turning around and re-impacting the Moon, but atoms launched into other trajectories can be given sufficient additional kinetic energy during their flight to ultimately escape, whereupon they are further accelerated away from the Sun and into the distant lunar Na tail [*Wilson et al.*, 1999].

[11] The apparent size of the lunar Na exosphere is a strong function of the Na atom ejection speeds from the surface. Figure 2 shows simulated images generated from three different monoenergetic exosphere models. The low speed exosphere in Figure 2a is closely confined to the lunar limb, while the entirely escaping high speed exosphere in Figure 2c is too extended. The model in Figure 2b very closely resembles the data.

[12] There are actually many different speed distributions that can fit the observed radial profile of the lunar exosphere besides the monoenergetic model in Figure 2b. To demonstrate the range of speed distributions that are consistent with the data, we choose two which represent extreme cases and generate lunar exosphere models for each. Model A uses the nearly monoenergetic distribution shown in Figure 2b, where the ejection speeds are evenly distributed between 2.2 and 2.3 km s^{-1}. Model B uses a distribution from 2.0 to 2.4 km s^{-1} that is weighted towards lower speeds, simulating the high speed tail of a broader distri-

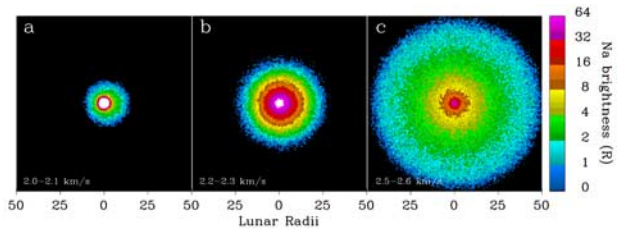

Figure 2. Images for three monoenergetic model Na exospheres (without the effect of the Earth's shadow) for an escape rate of 5 $\times$ 10^{21} atoms s^{-1}. The outer edge of the exosphere delineates the point at which the fastest atoms appear to "turn around" due to their acceleration away from the Earth via solar radiation pressure. (a) The lower-speed exosphere barely forms a tail, which is offset to the right of the Moon due to the Earth-Moon system's orbital motion to the east (left). (b) This exosphere very nearly matches the data. (c) This higher-speed exosphere is too bright at large distances and too dim near the Moon.

bution that peaks somewhere below 2 km s^{-1}. Figure 3 shows a comparison of the two speed distributions. Figure 4 shows that both of the sources yield profiles which are essentially indistinguishable from the radial profile of the observed exosphere shown in Figure 1.

[13] Although we cannot uniquely determine the exospheric speed distribution from this data, we can place some useful limits on the speeds. Comparisons of numerous model speed distributions with our data indicate that $\leq$20% of the escaping Na atoms are ejected from the surface with speeds above 2.3 km s^{-1}; in other words, relatively few, if any, of the escaping atoms are ejected from the surface with escape speed. Thus, solar radiation pressure is responsible for most of the neutral Na escape into the outer exosphere and Na tail.

[14] In order to reproduce the observed radial brightness profile of the exosphere, model A requires a Na ejection rate of 0.5×10^{22} atoms s^{-1} and model B requires 1.3×10^{22} atoms s^{-1}. These values are comparable to rates found previously from other data using similar simulations. *Wilson et al.* [1999] derived a nominal rate of 0.7×10^{22} atoms s^{-1} for speeds of 2.1 to 2.4 km s^{-1} from observations of the lunar Na tail at New Moon, and *Ip* [1991] calculated a rate of $\sim 10^{22}$ atoms s^{-1} for speeds of 2.0 to 2.4 km s^{-1}. *Flynn and Mendillo* [1995] and *Mendillo et al.* [1997] calculated total surface ejection rates of $1.4 - 3.5 \times 10^{22}$ Na atoms s^{-1} (not all of which escapes) from earlier eclipse and quarter Moon observations, assuming a thermal speed distribution for the exosphere with a temperature of 1400 K.

4. Discussion

[15] The Na atoms considered here are the fastest component of the lunar Na exosphere, and thus represent the most energetic space weathering processes acting on the lunar surface. This study therefore does not address any population of atoms liberated by thermal desorption. On the other hand, ion sputtering and electron or photon stimulated desorption are expected to eject some atoms with velocities >2 km s^{-1} [e.g., *Johnson and Baragiola*, 1991; *Madey et al.*, 1998; *Yakshinskiy and Madey*, 1999]. In addition, lunar Na tail observations following the Leonid meteor shower of 1998 showed empirically that impact-vaporization of meteors contributes to this Na-tail forming population [*Wilson et al.*, 1999].

[16] Our image of the full extent of the lunar Na exosphere provides a unique constraint on the high-end speed distribution of the lunar exosphere source processes by revealing the "turn-around" distance of the fastest exospheric atoms. Our results qualitatively agree with earlier observations, both within 1 R_M of the lunar limb [e.g., *Sprague et al.*, 1992] and further out [*Flynn and Mendillo*, 1993, 1995; *Mendillo et al.*, 1993, 1997], that indicate that the lunar Na exosphere is dominated by source speeds that are below the escape speed. Combining the results here with observations at other phases and spatial scales will ultimately help determine the relative importance of the various exosphere-generating mechanisms at the Moon's surface.

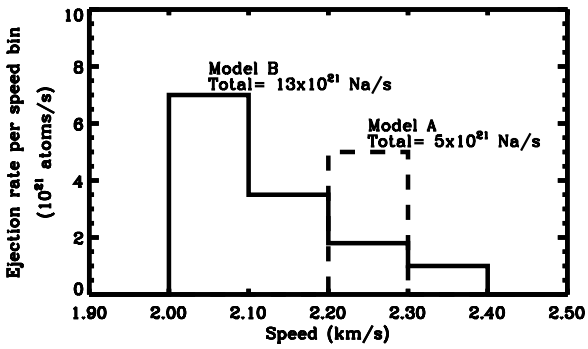

Figure 3. Surface ejection speed distributions for the two Na exospheric models. Model A is nearly monoenergetic, while model B resembles a high-speed tail of a broader distribution. Velocity bins are 0.1 km s^{-1} in size.

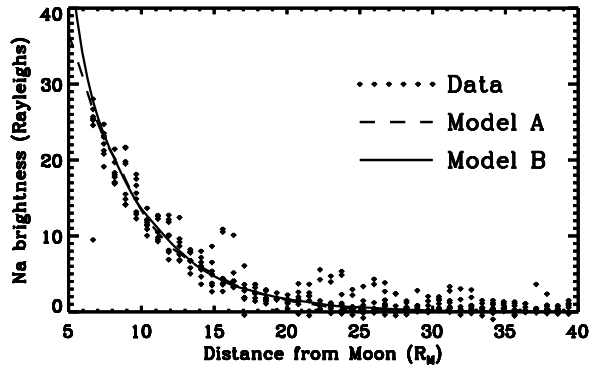

Figure 4. Comparison of radial profiles for the observed Na exosphere and the two model exospheres. The two model profiles are nearly indistinguishable and are good matches to the data. The brightness values for the data image are derived by dividing the image azimuthally into 8 pie-shaped sectors centered on the Moon, and averaging all pixels at a given radial distance within each sector. Thus, while the exospheric brightness decreases with increasing distance from the Moon, there are proportionately more pixels sampling those dimmer regions, making it possible to distinguish azimuthally-averaged brightnesses of only a few Rayleighs.

[17] **Acknowledgments.** We would like to thank Dr. Robert Robson and David Godwin of James Cook Univ., Cairns, Australia, and James Bak and Bob Dollery of the Cairns Astronomy Group for their valuable assistance with the observations. This work was supported, in part, by the NASA planetary astronomy program and seed research funds from the Center for Space Physics at Boston University.

References

Baumgardner, J., B. Flynn, and M. Mendillo, Monochromatic imaging instrumentation for application in aeronomy of the Earth and planets, *Opt. Eng.*, *32*, 3028–3032, 1993.

Combi, M. R., M. A. DiSanti, and U. Fink, The Spatial Distribution of Gaseous Atomic Sodium in the Comae of Comets: Evidence for Direct Nucleus and Extended Plasma Sources, *Icarus*, *130*, 336–354, 1997.

Contarini, G., C. Barbieri, G. Corrain, G. Cremonese, and R. Vio, Spectroscopic observations of the sodium atmosphere of the Moon, *Planet. Space Sci.*, *44*, 417–420, 1996.

Cremonese, G., and S. Verani, High resolution observations of the sodium emission from the Moon, *Adv. Space Res.*, *19*, 1561–1569, 1997.

Flynn, B., and M. Mendillo, A Picture of the Moon's Atmosphere, *Science*, *261*, 184–186, 1993.

Flynn, B., and M. Mendillo, Simulations of the lunar sodium atmosphere, *J. Geophys. Res.*, *100*, 23,271–23,278, 1995.

Huebner, W. F., Solar photo rates for planetary atmospheres and atmospheric pollutants, *Astrophys. and Space Sci.*, *195*, 1–294, 1992.

Hunten, D. M., R. W. H. Kozlowski, and A. L. Sprague, A possible meteor shower on the Moon, *Geophys. Res. Lett.*, *18*, 2101–2104, 1991.

Hunten, D. M., G. Cremonese, A. L. Sprague, R. E. Hill, S. Verani, and R. W. H. Kozlowski, The Leonid Meteor Shower and the Lunar Sodium Atmosphere, *Icarus*, *136*, 298–303, 1998.

Ip, W. H., The atomic sodium exosphere/coma of the Moon, *Geophys. Res. Lett.*, *18*, 2093, 1991.

Johnson, R. E., and R. Baragiola, Lunar Surface: Sputtering and Secondary Ion Mass Spectroscopy, *Geophys. Res. Lett.*, *18*, 2169–2172, 1991.

Madey, T. E., B. V. Yakshinskiy, V. N. Ageev, and R. E. Johnson, Desorption of alkali atoms and ions from oxide surfaces: Relevance to origins of Na and K in atmospheres of Mercury and the Moon, *J. Geophys. Res.*, *103*, 5873–5887, 1998.

Mendillo, M., B. Flynn, and J. Baumgardner, Imaging Experiments to Detect and Extended Sodium Atmosphere on the Moon, *Adv. Space. Res.*, *13*, 10,313–10,319, 1993.

Mendillo, M., and J. Baumgardner, Constraints on the origin of the Moon's atmosphere from observations during a lunar eclipse, *Nature*, *377*, 404–406, 1995.

Mendillo, M., J. Emery, and B. Flynn, Modeling the Moon's extended sodium cloud as a tool for investigating sources of transient atmospheres, *Adv. Space Res.*, *19*, 1577–1560, 1997.

Mendillo, M., J. Baumgardner, and J. K. Wilson, Observational Test for the Solar Wind Origin of the Moon's Sodium Atmosphere, *Icarus*, *137*, 13–23, 1999.

Potter, A. E., and T. H. Morgan, Extended sodium exosphere of the Moon, *Geophys. Res. Lett*, *15*, 1515–1518, 1988.

Potter, A. E., and T. H. Morgan, Observations of the lunar sodium exosphere, *Geophys. Res. Lett.*, *18*, 2089–2092, 1991.

Potter, A. E., and T. H. Morgan, Coronagraphic observations of the lunar sodium exosphere near the lunar surface, *J. Geophys. Res.*, *103*, 8581–8586, 1998.

Potter, A. E., R. M. Killen, and T. H. Morgan, Variation of lunar sodium during passage of the Moon through Earth's magnetotail, *J. Geophys. Res.*, *105*, 15,073–15,084, 2000.

Sprague, A. L., R. W. H. Kozlowski, D. M. Hunten, W. K. Wells, and F. A. Grosse, The sodium and potassium atmosphere of the Moon and its interaction with the surface, *Icarus*, *96*, 27–42, 1992.

Sprague, A. L., D. M. Hunten, R. W. H. Kozlowski, F. A. Grosse, R. E. Hill, and R. L. Morriss, Observations of sodium in the lunar atmosphere during International Lunar Atmosphere Week, 1995, *Icarus*, *131*, 372–381, 1998.

Stern, S. A., The lunar atmosphere: History, status, current problems, and context, *Rev. Geophys.*, *37*(4), 453–491, 1999.

Stern, S. A., and B. C. Flynn, Narrow-field Imaging of the Lunar Sodium Exosphere, *Astron. J.*, *109*, 835–841, 1995.

Tyler, A. L., R. W. H. Kozlowski, and D. M. Hunten, Observations of sodium in the tenuous lunar atmosphere, *Geophys. Res. Lett.*, *15*, 1141–1145, 1988.

Verani, S., C. Barbieri, C. R. Benn, G. Cremonese, and M. Mendillo, 1999 Quadrantids and the lunar Na atmosphere, *Monthly Notices of the Royal Astronomical Society*, *327*, 244–248, 2001.

Wilson, J. K., S. M. Smith, J. Baumgardner, and M. Mendillo, Modeling an Enhancement of the Lunar Sodium Atmosphere and Tail During the Leonid Meteor Shower of 1998, *Geophys. Res. Lett.*, *26*, 1645–1648, 1999.

Yakshinskiy, B. V., and T. E. Madey, Photon-stimulated desorption as a substantial source of sodium in the lunar atmosphere, *Nature*, *400*, 642–644, 1999.

J. K. Wilson, Center for Space Physics, Boston Univ., 725 Commonwealth Ave., Boston, MA 02215, USA. (Jkwilson@bu.edu)

J. Baumgardner and M. J. Mendillo, Center for Space Physics, Boston Univ., USA.